

LETTER • OPEN ACCESS

Global-scale changes to extreme ocean wave events due to anthropogenic warming

To cite this article: Joao Morim *et al* 2021 *Environ. Res. Lett.* **16** 074056

View the [article online](#) for updates and enhancements.

You may also like

- [Extreme Wave Height Analysis in Natuna Sea Using Peak-Over Threshold Method](#)
Ismail Abdul Jabbar and Nining Sari Ningsih
- [Roadmap on optical rogue waves and extreme events](#)
Nail Akhmediev, Bertrand Kibler, Fabio Baronio et al.
- [Magnetic Waves Excited by Newborn Interstellar Pickup Ions Measured by the Voyager Spacecraft from 1 to 45 au. I. Wave Properties](#)
Sophia J. Hollick, Charles W. Smith, Zackary B. Pine et al.

ENVIRONMENTAL RESEARCH
LETTERS

LETTER

Global-scale changes to extreme ocean wave events due to anthropogenic warming


OPEN ACCESS

RECEIVED
12 January 2021REVISED
22 June 2021ACCEPTED FOR PUBLICATION
30 June 2021PUBLISHED
16 July 2021

Original content from this work may be used under the terms of the [Creative Commons Attribution 4.0 licence](#).

Any further distribution of this work must maintain attribution to the author(s) and the title of the work, journal citation and DOI.



Joao Morim^{1,2,*}, Sean Vitousek², Mark Hemer¹, Borja Reguero³, Li Erikson², Merce Casas-Prat⁴, Xiaolan L Wang⁴, Alvaro Semedo⁵, Nobuhito Mori⁶ , Tomoya Shimura⁶, Lorenzo Mentaschi⁷ and Ben Timmermans⁸

¹ Commonwealth Scientific and Industrial Research Organisation (CSIRO) Oceans and Atmosphere, Hobart, TAS, Australia

² US Geological Survey (USGS), Pacific Coastal and Marine Science Center, Santa Cruz, CA, United States of America

³ Institute of Marine Sciences, University of California, Santa Cruz, CA, United States of America

⁴ Environment and Climate Change Canada, Climate Research Division, Toronto, ON, Canada

⁵ IHE Delft Institute for Water Education, Delft, The Netherlands

⁶ Disaster Prevention Research Institute, Kyoto University, Kyoto, Japan

⁷ European Commission, Joint Research Centre (JRC), Ispra, Italy

⁸ Climate and Ecosystems Science Division, Lawrence Berkeley National Laboratory (LBNL), Berkeley, CA, United States of America

* Author to whom any correspondence should be addressed.

E-mail: joao.morimnascimento@griffithuni.edu.au

Keywords: ocean waves, global warming, climate extremes, southern annular mode

Supplementary material for this article is available [online](#)

Abstract

Extreme surface ocean waves are often primary drivers of coastal flooding and erosion over various time scales. Hence, understanding future changes in extreme wave events owing to global warming is of socio-economic and environmental significance. However, our current knowledge of potential changes in high-frequency (defined here as having return periods of less than 1 year) extreme wave events are largely unknown, despite being strongly linked to coastal hazards across time scales relevant to coastal management. Here, we present global climate-modeling evidence, based on the most comprehensive multi-method, multi-model wave ensemble, of projected changes in a core set of extreme wave indices describing high-frequency, extra-tropical storm-driven waves. We find changes in high-frequency extreme wave events of up to ~50%–100% under RCP8.5 high-emission scenario; which is nearly double the expected changes for RCP4.5 scenario, when globally integrated. The projected changes exhibit strong inter-hemispheric asymmetry, with strong increases in extreme wave activity across the tropics and high latitudes of the Southern Hemisphere region, and a widespread decrease across most of the Northern Hemisphere. We find that the patterns of projected increase across these extreme wave events over the Southern Hemisphere region resemble their historical response to the positive anomaly of the Southern Annular Mode. Our findings highlight that many countries with low-adaptive capacity are likely to face increasing exposure to much more frequent extreme wave events in the future.

1. Introduction

Extratropical-generated extreme ocean waves affect coastal processes, natural ecosystems, and populations [1, 2], being often main drivers of coastal recession, elevated coastal water levels (via wave setup and swash) [3] and flooding [4]. Global-scale analyses have assessed how global ocean wind-wave fields may respond to scenarios of increased anthropogenic

forcing [5]. The majority address changes in global mean wave conditions, and only a few consider changes in extreme wave climatology [5]. These few analyses on future extremes explore projected changes in the magnitude of annual maximum significant wave height and low-frequency (≥ 20 years return period) extreme wave events [6–9]. Nevertheless, global simulations of low-frequency extreme (both surface wind and waves)

events vary widely across contemporary global climate models (GCM) [7, 10] and exhibit a suboptimal representation of the magnitude of extreme events (e.g. owing to their limited resolution) [10, 11]. In addition, extreme value analysis of projected future significant wave height (H_s)—used to estimate long-return periods, introduces an uncertainty which generally exceeds that of long-term climatic trends [12]. Consequently, projections of low-frequency extreme wave events are unlikely to detect a reliable signal of change, a signal which stands out from natural climate variations and is consistent among climate models [13].

So far, projected changes in the magnitude and frequency of extreme extra-tropical storm-driven wave events occurring more than once per year (hereafter ‘high-frequency extreme waves’) received little, to no, attention. In addition to being inherently much better resolved by global models relative to low-frequency events, such events can severely erode coastlines and are more directly relevant to coastal wave-driven risks (e.g. coastal erosion and flooding) at management time scales [14, 15]. For instance, the number and persistence of high-frequency extreme wave events can strongly influence shoreline-position changes [16–18], with its induced recession up to 2–5 orders of magnitude greater than long-term erosion [18]. Most importantly, accelerated sea-level rise will continuously reduce elevation differences between our coastal waterline and infrastructures [19, 20], therefore allowing lower-magnitude high-frequency wave events to progressively exceed flooding thresholds [19, 20].

Here we quantify, for the first time, the robustness in high-frequency extreme wave events projection using a broad set of coastal-impact-relevant wave indices (section 2) proposed by the World Climate Research Program (WCRP) Expert Team on Climate Change Detection and Indices (ETCCDI) [21]. The detailed definitions of the ETCCDI extreme wave indices are provided in section 2. Similar indices related to atmospheric and land variables (e.g. temperature, streamflow, and precipitation) [22] form the core knowledge of climate extremes described by the Intergovernmental Panel on Climate Change (IPCC) [23]. However, the application of ETCCDI extreme indices to assess ocean extreme wave events has remained thus far unexplored. The projected changes in the ETCCDI extreme indices are based on a very large community-based ensemble of global wave projections [24, 25] covering a range of future greenhouse-gas emission scenarios, GCM model forcing and wave-downscaling approaches. The different GCM forcing and wave modelling approaches in the ensemble vary in their representation of the projected changes (i.e. in intensity, frequency, and distribution of extreme-driven ocean wave events). Therefore, the research presented herein provides a much wider sampling of total projection uncertainty compared

to past research to date focusing on low-frequency storm wave events from climate-model-driven simulations.

2. Data and methods

2.1. ETCCDI extreme wave indices

The joint CCI/WCRP-CLIVAR/JCOMM ETCCDI [26] developed a set of extreme climate indices (for variables such as temperature, or precipitation) to support climate change detection and attribution [21, 26]. In addition to these, a set of extreme ocean wave height indices were also developed by the ETCCDI commission which are used in this analysis:

2.1.1. Threshold-based indices

- (a) Rough wave days: annual count of days when daily-max $H_s > 2.5$ m (days)
- (b) High wave days: annual count of days when daily-max $H_s > 6$ m (days)

2.1.2. Percentile distribution-based indices

- (c) Frequency of low (low-decile-days) days: annual frequency of days when daily max $H_s < 10$ th percentile (%) over present-day baseline period;
- (d) Frequency of high (top-decile-days) days: annual frequency of days when daily max $H_s > 90$ th percentile (%) over present-day baseline period;

2.1.3. Percentile- and duration-based indices

- (e) (Top-decile) Wave-spell-storm duration: annual count of days with at least two consecutive days when daily max $H_s > 90$ th percentile (days) over present-day baseline period.

These indices described above summarize key extreme ocean wave characteristics that are internationally agreed as important for analysis of changes in climate extremes [21, 23]. We note that although some of the (ETCCDI) extreme indices do not fully align with the ‘conventional’ definition of low-frequency extremes (i.e. recurring across multi-decadal to centennial time-scales), they can generally be used within a wide socio-economic and scientific context. For instance the wave-storm-spell duration index describes storm ocean wave events lasting two consecutive days, therefore capturing two peak semi-diurnal tide cycles when wave-driven flooding is most likely.

2.2. COWCLIP global wave ensemble data and skill

We used 80 members of the COWCLIP2.0 global wave ensemble [24, 25] (i.e. all members with available ETCCDI extreme indices) to calculate projected changes in high-frequency extreme wave events. The ensemble members contain statistical and dynamical simulations over the representative present-day (1981–2004) and future (2081–2100) time-slices for RCP4.5 and RCP8.5 scenarios at 1° resolution. A brief

description of the COWCLIP2.0 ensemble members used is provided within supplementary information, with their details provided in the original dataset descriptor [24, 25].

The ensemble used has been extensively compared against different sources of ocean wave data [24, 25] for different H_s statistics (such as mean and high-percentiles) at annual and seasonal time-scales [24, 25]. Some of its wave members have been also previously used to assess changes to annual maximum and centennial time-scale extreme wave events (i.e. return period ≥ 50 years [7–9]). Here we compare the COWCLIP multi-member ensemble mean of rough wave days, high wave days, and wave-storm-spell duration against those obtained from the ERA5 wave reanalysis (here ERA5) [26] for the present-day period (1979–2004). We present this comparison using Taylor diagrams [27] which exhibit spatial correlation (SC), normalized standard deviation (NSD) and centered-root-mean-square-difference (CRMSD) within a single figure, following the IPCC climate model evaluation guidelines [28, 29]. To further support and contextualize this model skill analysis, we also compare the COWCLIP multi-member ensemble mean against five different global wave hindcast products (including a new global wave hindcast—named here ECMWF-ERA5—forced with ERA5 surface winds and sea ice forcing) that are extensively documented and/or validated [30–34]. A brief description of these global wind-wave products is provided within the supplementary information.

2.3. CMIP5 global wind ensemble

We used daily-max wind speeds from the 20 CMIP5 climate models (available in the WCRP CMIP5 archive) which were used to force the global wave simulations over the periods 1979–2005 and 2081–2100 for RCP8.5. These are all the GCM models that provide daily-max wind speeds. Some GCM models do not provide daily-max surface wind speed (e.g. ACCESS1.0 and ACCESS1.3) but have sub-daily wind components (from which we calculate daily-max surface wind speeds). The statistically-downscaled members from ECCO(s) were obtained using sea-level pressure (SLP) fields (and have not been considered here for simplicity). Instead, we use their respective surface winds. The skill (and associated uncertainty) of the CMIP5 ensemble members to represent extreme wind speed values (such as 99th percentile of daily-maximum wind speeds) at global and regional-scales has been extensively described elsewhere [10, 35].

2.4. Future projected changes

Future projected changes in ETCDDI extreme wave indices (except for high wave days) and in surface wind speeds were derived as a relative change between historical-day (1979–2004) and the future

(2081–2100) time-slices for each model ensemble member following previous analysis [25]:

$$\Delta_{j,k} = \frac{\bar{H}_{j,k}^{\text{Future}} - \bar{H}_{j,k}^{\text{Present-day}}}{\bar{H}_{j,k}^{\text{Present-day}}} \quad (1)$$

where $\Delta_{j,k}$ is the projected change for a given ETCDDI index at grid node k by the GCM model j . Since projected relative changes in significant wave height are strongly dependent on GCM-forcing [25] (surface winds and pressure fields from which the wave field originates), a weighted multi-member ensemble mean was derived by applying a weighting factor to each member:

$$\bar{x} = \frac{\sum_{i=1}^n (\Delta_{i,\delta} - W_{i,\delta})}{\sum_{i=1}^n W_{i,\delta}} \quad (2)$$

where $\Delta_{i,\delta}$ is the projected change for a given ETCDDI index δ by the ensemble member i , and $W_{i,\delta}$ is the weighting factor for ensemble member i for that same index (calculated as the number of ensemble members with that same forcing GCM amongst all members n). We also derived a uniformly weighted ensemble mean and obtained similar results.

2.5. Robustness

We adopted a methodology [36] advised by the IPCC Assessment Report Working Group 1 to establish areas of robustness. This methodology is considered a suitable, effective method because, unlike other criteria, such method does not omit internal climate variability and is able to detect areas with lack of inter-member agreement and/or lack of climate signal (by assessing the consensus on the significance of projected changes) [36].

Here, we evaluated the significance of change projected by each of the ensemble members individually, using a two-tailed Welch's t -test that allows for different variances between the present-day and future periods. The test was performed at the 5% significance level. In order to define regions of robust projected changes, we first identified areas (i.e. grid cells) where 50% or more of the ensemble members projected a significant change. Within these regions, we further identified the locations where 90%, or more, of the ensemble members exhibiting a significant change agreed on the sign of the projected future changes; these are the regions of robust changes projected by the multi-member ensemble mean, and are hatched in figure 2 and supplementary figure S3 (available online at stacks.iop.org/ERL/16/074056/mmedia). Here, we used a higher threshold (90%) than the standard 80% [36] for inter-member agreement on the direction of climate change. We applied the robustness criterion to the COWCLIP ensemble of wind-wave simulations and to the CMIP5 ensemble of surface wind speeds. The key findings are consistent of other IPCC-referenced

methods are used. To further improve the robustness assessment [36], we also tested that, within all regions of robustness, the ensemble-mean projected changes is statistically significant using the one-sample Student t -test at the 5% significance level.

2.6. SAM index from reanalysis and climate models

We derived the high wave days and wave-storm-spell duration indices from the ERA5 global wave reanalysis [26] and also from the COWCLIP models to understand their historical response to the polarity phases of the SAM. The gridded hourly time-series of H_s (spanning from 1979 to 2017) derived from the ERA5 were used to calculate the annual time series of high wave days and wave-storm-spell duration following that same method [24] applied to the COWCLIP global wave ensemble (section 2.2). Based on the time series of high wave days and wave-storm-spell duration derived from the ERA5 data and those from the COWCLIP models, we assessed the changes in the ETCDDI extreme wave indices during both the positive and negative phase anomalies of the SAM mode compared to the long-term baseline mean. The approaches used to define positive and negative phases of the SAM are described below.

We estimated the SAM index using the ERA5 monthly SLP data in the historical period 1979–2017 following a previously established methodology [37, 38]. We standardized the SAM index by removing the mean and dividing it by the standard deviation calculated over the period 1979–2004 to be consistent with the time slice period of the GCM-driven wave simulations (section 2.6.2). We smoothed the standardized SAM index using a 6 month running-average filter so that solely interannual variations in the SAM mode was captured. We also tested other high-pass filters, and obtained consistent findings. We then identified the strongest positive and negative SAM anomalies when the index exceeded +1.0 and –1.0 during at least 3 consecutive months, respectively. Years with strong positive and negative anomalies were not considered for consistency. We detected 10 years of strong negative SAM and 11 years of strong positive SAM mode (supplementary figure S1). We tested the results using an even number of years by removing the year with weakest positive SAM index out of the original 11 and the results are consistent. These years were used to calculate the annual mean of high wave days and wave-storm-spell-duration during positive and negative SAM, respectively (and the change relative to the historical baseline mean over 1979–2017).

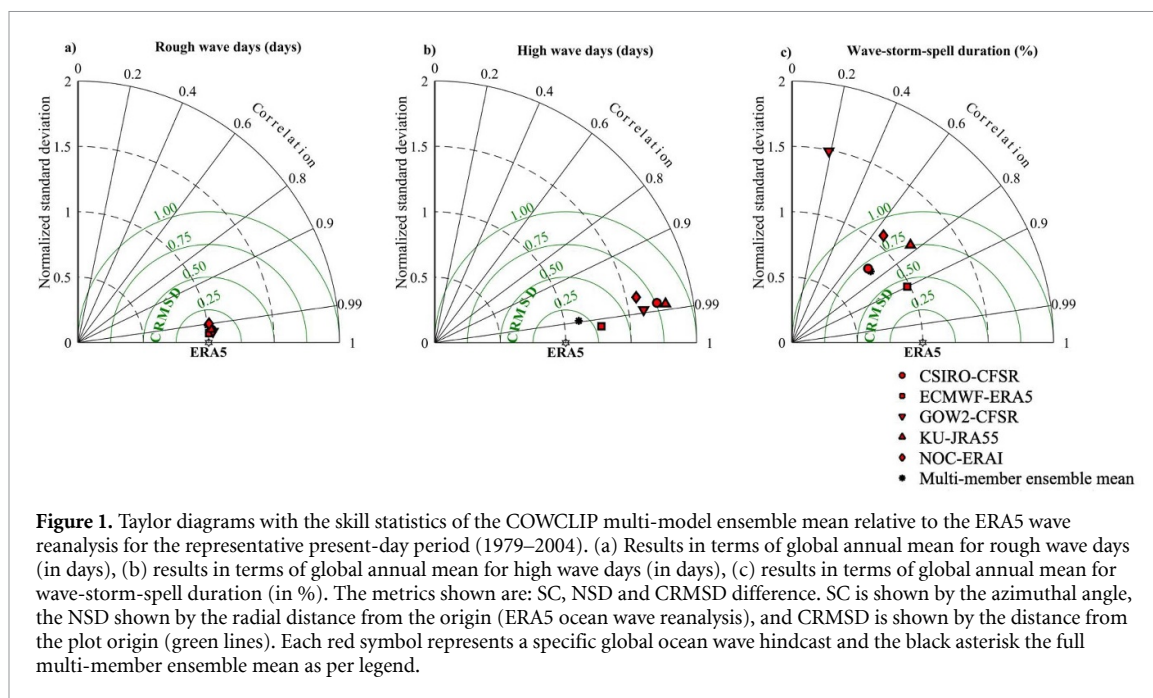
We computed the SAM index (across the present-day period 1979–2004) for the different climate models using their respective monthly time series of SLP data. Note that the period of present-day simulations does not need to match the historical period of ERA5 reanalysis, as climate models are not in temporal phase with the observed natural climate variability.

It is worth noting that the SLP data was extracted from the specific GCM realizations (ensemble member which defines the GCM initial state) used to force the respective global ocean wave simulations, as reported in the wave ensemble. We also excluded the member from the ECCC(s) ensemble forced by the FGOALS-S2 model because we could not find access to its sea level pressure data within the CMIP5 archive. In addition, we excluded all the members forced by the EC-EARTH model as there is no documentation on their respective realization details. We obtained the SAM index using monthly SLP data over the present-day period 1979–2004 from the respective CMIP5 climate models following the same method used for the ERA5 data [38].

3. Results

3.1. Global wave ensemble skill

As previously described (see section 2.2.1), we compare the present-day ensemble mean of rough wave days, high wave days, and wave-storm spell duration, against different reference global wave datasets via Taylor diagrams [27], thus providing SC, NSD and CRMSD skill statistics. The ensemble exhibits an overall relatively good agreement relative to ERA5 for rough wave days, high wave days and wave-storm-spell duration. CRMSD values for rough and high wave days are always below ~ 0.25 m, NSD under ~ 0.5 m and SC values above ~ 0.95 (figure 1). The skill metrics exhibited by the ensemble mean (and the global wave hindcasts) are slightly lower in for the wave-storm-spell duration index (0.65, 0.25, and 0.80, respectively) due to the intrinsic characteristics of this index (such as its unit scale). The model skill metrics presented here are comparable to prior skill analysis of extreme wave and wind statistics [11, 12, 24, 25] based on CMIP5 models. For instance, in terms of representing global and regional annual mean values of 99th percentile H_s , the COWCLIP multi-member ensemble mean exhibits similar skill statistics with CRMSD and NSD values ranging 0.25–0.50 m and SC values ranging 0.95–0.98 [24, 25]. The model skill metrics described here are also within the range of model skill statistics reported in terms of GCM models representing atmospheric and terrestrial variables based on ETCDDI extreme indices [22, 39]. In addition, we find the wave ensemble skill is well within the range of uncertainty found among contemporary global wave hindcasts as illustrated in figure 1, therefore providing confidence that this wave ensemble is overall representative of these widely used global wave products (figure 1). The relatively good agreement between the multi-member ensemble mean and the ERA5 wave reanalysis is consistent with the ETCDDI extreme wave indices being much less sensitive to the well-documented misrepresentations of the peak of extreme events by wave models, given that they do not attempt to resolve



the precise magnitude of the extreme wave peaks (as attempted by analysis of low-frequency storm wave events based on extreme value analysis [6–9]).

3.2. Global projected changes

The projected changes in high-frequency ocean extreme wave events by the end of the 21st century period are assessed under two representative concentration pathways (RCP): a mild-stabilizing RCP4.5 scenario and a high-level emission RCP8.5 scenario. We find that projected future changes in these ETCCDI extreme wave indices exhibit well-defined large-scale spatial patterns of change (figure 2), with strong latitudinal dependence (supplementary figure S2). The patterns of changes under RCP4.5 and RCP8.5 are extremely consistent (figure 2), however, the global ocean exhibiting robust changes is much larger for RCP8.5. In addition, the magnitude of projected changes is considerably greater for RCP8.5 almost everywhere. When averaged globally, projected changes in rough wave days, high wave days wave-storm-spell duration for RCP8.5 exceed those of the RCP4.5 by ~100%, 80% and 110% respectively (supplementary figure S3). In specific areas of the Southern Ocean, changes in high wave days and wave-storm-spell duration for RCP8.5 are up to ~150%–200% greater than corresponding projected changes for RCP4.5 scenario (supplementary figure S3).

Specifically focusing on RCP8.5, we show that projected changes in high-frequency extreme wave events present strong inter-hemispheric asymmetry (figure 2 and supplementary figure S2) with projected increases in the high-frequency ocean extreme wave events in the Southern Hemisphere and general decrease in the Northern Hemisphere.

In the Southern Hemisphere, there is a robust zonally-uniform increase in the rough wave days (~5%–10%), high wave days (~5–30 d) and wave-storm-spell duration (~10%–50%) within high-latitude regions (>50° S). Changes in rough wave days are relatively small (~5%) over these latitudes (>50° S), as wave conditions >2.5 m persist almost continuously even in the representative present-day period (figure 2(a)). In the mid-latitude areas of the Southern Ocean region (30°–50° S), a robust projected decrease is seen in rough wave days (5%–10%) and wave-storm-spell-duration (25%–50%). There is also a projected future decrease in the high wave days in this region (~5–10 d) but lack robustness. The mid-latitude projected decrease in the Southern Ocean also becomes clearly visible when changes are zonally-averaged (supplementary figure S2). We find a robust increase in the wave-storm-spell duration in the tropical Southern Hemisphere (0°–30° S). The increase in wave-storm-spell duration is also found robust over some areas of the Atlantic Ocean and in the Eastern Pacific Ocean (off Central and South America) where projected increases reach to ~50%–100% (figure 2(c)).

In the Northern Hemisphere, we find robust projected decreases in rough wave days (~10%–30%) and wave-storm-spell duration (~10%–20%) across the North Atlantic, Mediterranean Sea and widespread regions within the North Pacific. The exception to the general decline in the high frequency extreme waves is found in the northern central Pacific, where there is a slight but not robust projected increase (figure 2(c)). The results for low and high wave days are overall consistent with the large-scale patterns of change previously described (see figure 2), although projected changes in frequency of low days

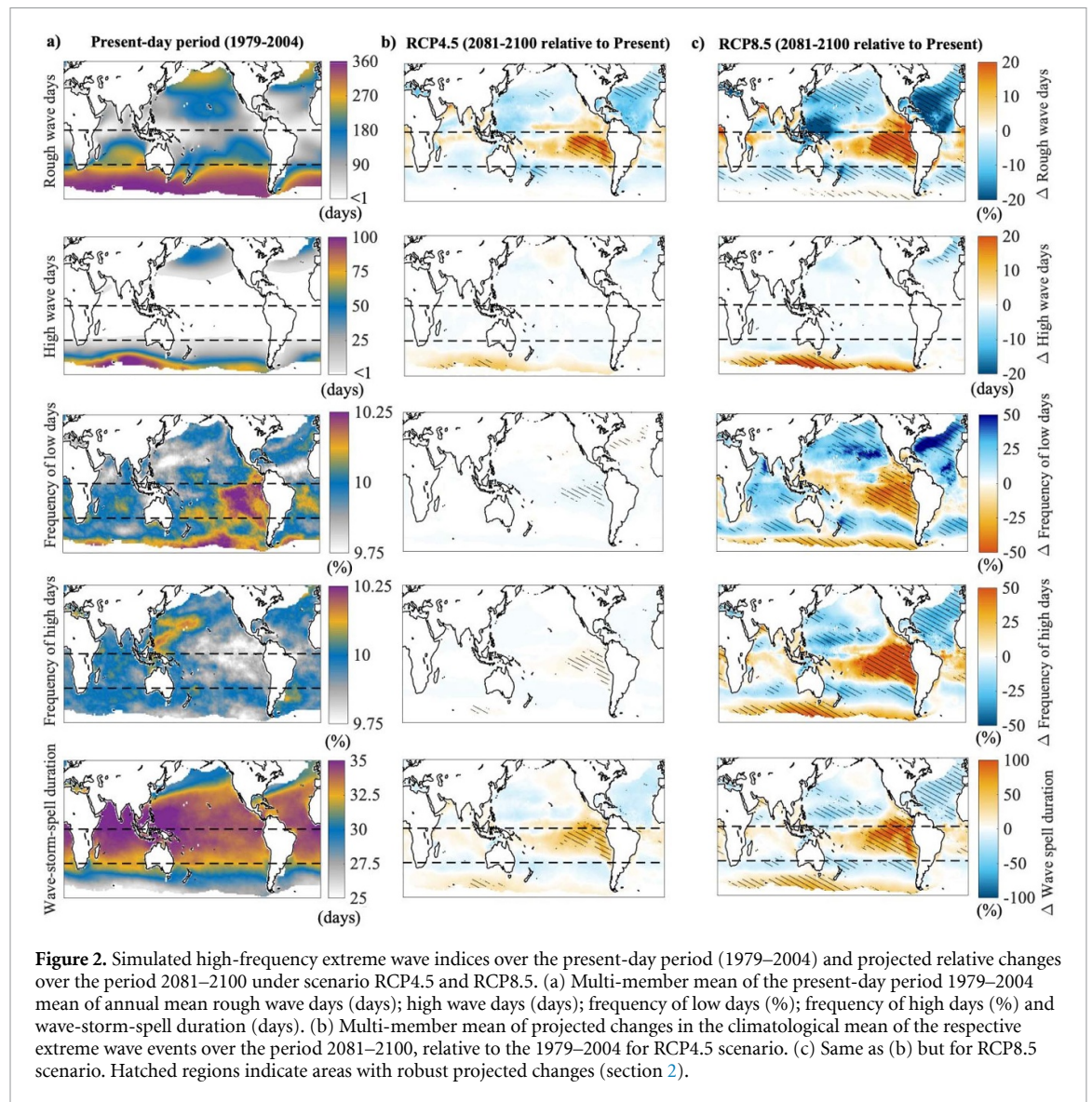


Figure 2. Simulated high-frequency extreme wave indices over the present-day period (1979–2004) and projected relative changes over the period 2081–2100 under scenario RCP4.5 and RCP8.5. (a) Multi-member mean of the present-day period 1979–2004 mean of annual mean rough wave days (days); high wave days (days); frequency of low days (%); frequency of high days (%) and wave-storm-spell duration (days). (b) Multi-member mean of projected changes in the climatological mean of the respective extreme wave events over the period 2081–2100, relative to the 1979–2004 for RCP4.5 scenario. (c) Same as (b) but for RCP8.5 scenario. Hatched regions indicate areas with robust projected changes (section 2).

exhibit a reversed pattern compared to the other extreme indices. This indicates that the increase in the frequency of low wave days occurs in part at the expense of high wave days.

We show that projected changes in the ETCDDI extreme wave indices previously described (figure 2) are strongly linked to the patterns of change found in ocean extreme wind speeds as shown by the forcing CMIP5 ensemble (figure 3). These findings are consistent with large-scale patterns of change exhibited by previous analysis [40]. The nearly uniform-decrease in the high-frequency extreme wave indices across most of the Northern Hemisphere is consistent with the general decrease in the extreme wind speeds over this region [40]. The patterns of projected future changes in the high-frequency extreme wave indices across the Southern Hemisphere are also in strong agreement with the poleward shift/rotation of the extra-tropical storm belt manifested through decreases and increases of extreme wind speeds across the mid-latitude (30° – 50° S) and high latitudes

($>50^{\circ}$ S), respectively. The results are consistent with projected changes in the extra-tropical mid-latitude storm track activity [41–43].

In further analysis, we demonstrate that, in Southern Hemisphere (where there is projected robust increase in the ETCDDI extreme indices), the patterns of projected change in the high wave days and wave storm spell duration (i.e. representing large and persistent storm wave events) strongly resemble their (historical) spatial response to the positive phase anomaly of the southern annular mode (SAM), as described by the ERA5 reanalysis (cf figures 2 and 4). See supplementary information for an extended discussion on the similar response of high wave days and wave-storm-spell duration to the phases of the SAM as described by the ERA5 wave reanalysis and the COWCLIP ensemble-mean (supplementary figure S5). The similarity between the patterns of projected changes in these extreme wave indices and their historical response to the SAM is evidently noticeable across most regions with robust projected changes

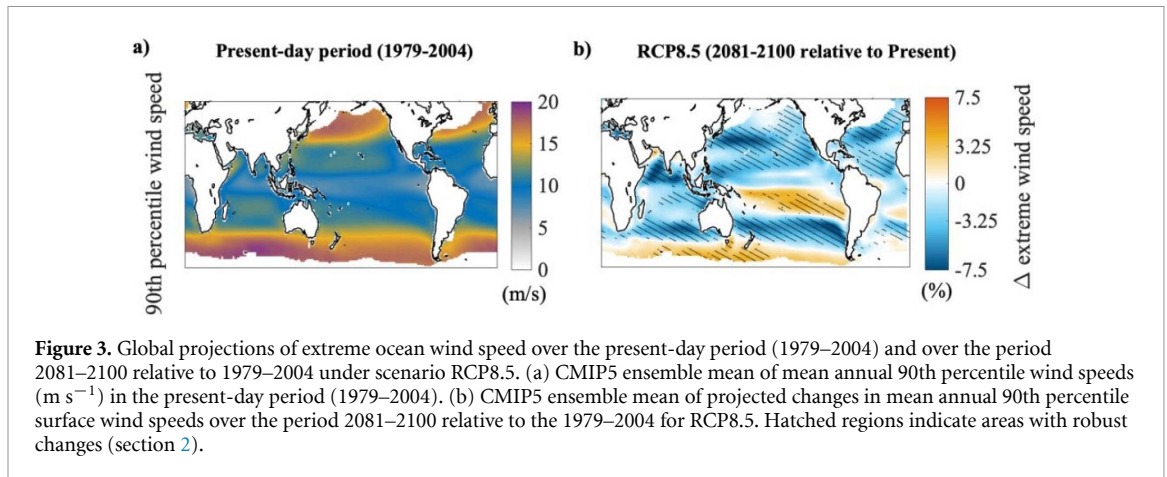


Figure 3. Global projections of extreme ocean wind speed over the present-day period (1979–2004) and over the period 2081–2100 relative to 1979–2004 under scenario RCP8.5. (a) CMIP5 ensemble mean of mean annual 90th percentile wind speeds (m s^{-1}) in the present-day period (1979–2004). (b) CMIP5 ensemble mean of projected changes in mean annual 90th percentile surface wind speeds over the period 2081–2100 relative to the 1979–2004 for RCP8.5. Hatched regions indicate areas with robust changes (section 2).

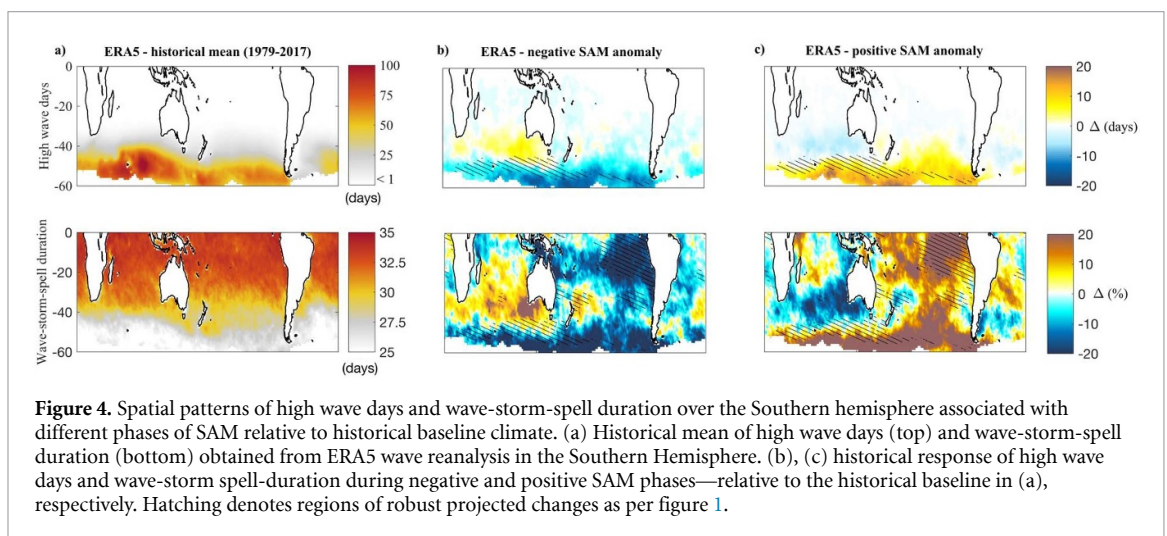


Figure 4. Spatial patterns of high wave days and wave-storm-spell duration over the Southern hemisphere associated with different phases of SAM relative to historical baseline climate. (a) Historical mean of high wave days (top) and wave-storm-spell duration (bottom) obtained from ERA5 wave reanalysis in the Southern Hemisphere. (b), (c) historical response of high wave days and wave-storm spell-duration during negative and positive SAM phases—relative to the historical baseline in (a), respectively. Hatching denotes regions of robust projected changes as per figure 1.

within the Southern Hemisphere (i.e. where there is strong confidence in results) (figure 4).

In regions without robustness, we also find a general agreement, yet with a few exceptions. This is the case of a specific mid-latitude region of the central South Pacific, where there is a projected decrease in the wave storm spell duration (figure 2(c)), whereas its historical response shows a relative increase during positive SAM anomaly (figure 4(c)). In this area, the shift is clear in the zonal wind patterns and mean SLP fields during strongly positive SAM events [44], but is not apparent in the extreme wave field owing to the increased equatorward propagation of swell events from the Southern Ocean to the tropics as previously documented [45].

In the tropical regions of the Southern Hemisphere ($>15^\circ$ S), projected changes are generally consistent with the intensification of the SAM. In the Eastern Southern Pacific, the projected robust increase in the wave-storm-spell duration is likewise consistent with the regional-scale intensification of ocean extreme wind speeds as described (see figure 3) and documented [45]. The results demonstrate that projected changes in high-frequency extreme wave

events are likely driven by a shift of the SAM towards its positive phase, which is consistent with the recently observed positive trend of the SAM mode in the past few decades [37, 38]. They are also in strong agreement with the projected positive and significant trend in the SAM shown by the CMIP5 multi-model ensemble over the 21st century [46–48].

4. Conclusions

This study presents 21st century projections of high-frequency extreme ocean wave events for RCP4.5 and RCP8.5 scenarios, with projected changes in the occurrence of these events almost doubling for the high-emission scenarios. For RCP8.5, there will be robust changes in extreme wave events across $\sim 30\%$ – 40% of the global ocean. Our findings reveal a strong inter-hemispheric asymmetry, with up to $\sim 50\%$ – 100% increases in extreme, persistent wave events (i.e. wave-storm-spell duration) over the low and high-latitudes of the Southern Hemisphere and $\sim 20\%$ – 50% decrease across the Northern Hemisphere. The projected changes described are over many regions considerably greater than projected

changes in extreme wave events at decadal to centennial time-scales (<20% along most the world's coastlines). We find the global distribution of projected change in high-frequency extreme wave events resemble, in general, the projected changes of extreme surface wind speeds. In the Southern Hemisphere, the region where wave-driven coastal hazards are expected to be exacerbated, our findings indicate that projected changes in high-frequency extreme wave events are likely associated with a future change in the SAM towards its positive phase, in agreement with projections of SAM for the 21st century period.

This study provides a new perspective on projected future changes in extreme ocean waves by quantifying change in high-frequency extreme wave events over decision/impact-relevant time horizons using a multi-index approach and a large multi-method multi-model ensemble. The projected increases in high-frequency extreme wave forcing across most of the Southern Hemisphere present broad-scale implications for many coastal countries that face increasing threats from coastal hazards. This is the case of Australia and New Zealand and also of many regions with low-adaptive capacity, such as the low-lying Pacific atolls and the western coasts of Central-South America and Central Africa where such events are already strongly linked to widespread coastal flooding and erosion [3, 49, 50]. The expected increase in these extreme wave events will likely exacerbate coastal impacts, atop impacts of sea-level rise [51]. More frequent sustained storm wave days are likely to impact capacity of coastlines to recover, exacerbating erosion patterns, and hence increasing coastal risks and the needs of adaptation these regions.

Whilst our results have far-reaching implications from many perspectives, they address only climate-driven changes in offshore extreme H_s events based on the ETCCDI indices developed by the WCRP Expert Team. It is important to explore how the other components of the ocean wave climate fields associated with such events might change, such as peak wave period and directions [52]. Also, we highlight the ongoing challenge of resolving the frequency of extreme wave events driven by intense tropical cyclones in the current global wave simulations forced directly with surface fields from CMIP5 models [53]. Is it expected that such issue could be better resolved using the next generation of GCMs. In the future, GCMs and downscaled global wind-wave projections may potentially provide a more robust insight on the magnitude, frequency, and/or duration of multidecadal to centennial-scales extreme events. However, our findings draw attention for urgent consideration of high-frequency extreme wind-wave forcing, as we look towards enhanced broad-scale assessments of coastal risk-hazard, adaptation and vulnerability from the scientific community [54].

Data availability statement

The CMIP5-driven wave data (COWCLIP2.0 dataset) is published via the Australian Ocean Data Network (AODN).

The metadata record is available via GeoNetwork at DOI: 10.26198/5d91a9d00d60d.

The dataset is accessible via the AODN THREDDS server (netCDF files) and can be accessed remotely using the OPeNDAP protocol at: <http://thredds.aodn.org.au/thredds/catalog/CSIRO/Climatology/COWCLIP2/catalog>.

ORCID iD

Nobuhito Mori  <https://orcid.org/0000-0001-9082-3235>

References

- [1] Toimil A, Losada I J, Nicholls R J, Dalrymple R A and Stive M J F 2019 Addressing the challenges of climate change risks and adaptation in coastal areas: a review *Coast. Eng.* **156** 103611
- [2] Hoeke R K, McInnes K L, Kruger J C, McNaught R J, Hunter J R and Smithers S G 2013 Widespread inundation of Pacific islands triggered by distant-source wind-waves *Glob. Planet. Change* **108** 128–38
- [3] Melet A, Meyssignac B, Almar R and Le Cozannet G 2018 Under-estimated wave contribution to coastal sea-level rise *Nat. Clim. Change* **8** 234–9
- [4] Melet A, Almar R, Hemer M, Le Cozannet G, Meyssignac B and Ruggiero P 2020 Contribution of wave setup to projected coastal sea level changes *J. Geophys. Res. Oceans* **125** e2020JC016078
- [5] Morim J, Hemer M, Cartwright N, Strauss D and Andutta F 2018 On the concordance of 21st century wind-wave climate projections *Glob. Planet. Change* **167** 160–71
- [6] Meucci A, Young I R, Hemer M, Kirezci E and Ranasinghe R 2020 Projected 21st century changes in extreme wind-wave events *Sci. Adv.* **6** 24
- [7] Wang X L, Feng Y and Swail V R 2014 Changes in global ocean wave heights as projected using multimodel CMIP5 simulations *Geophys. Res. Lett.* **41** 1026–34
- [8] Mentaschi L, Vousdoukas M I, Voukouvalas E, Dosio A and Feyen L 2017 Global changes of extreme coastal wave energy fluxes triggered by intensified teleconnection patterns *Geophys. Res. Lett.* **44** 2416–26
- [9] Lobeto H, Menendez M and Losada I J 2021 Future behavior of wind wave extremes due to climate change *Sci. Rep.* **11** 7869
- [10] Kumar D, Mishra V and Ganguly A R 2015 Evaluating wind extremes in CMIP5 climate models *Clim. Dyn.* **45** 441–53
- [11] Samayam S, Lafage V, Annamalaisamy S S, Arena F, Vallam S and Gavrilovich P V 2017 Assessment of reliability of extreme wave height prediction models *Nat. Hazards Earth Syst. Sci.* **17** 409–21
- [12] Vanem E 2015 Uncertainties in extreme value modelling of wave data in a climate change perspective *J. Ocean Eng. Mar. Energy* **1** 339–59
- [13] Knutti R and Sedláček J 2013 Robustness and uncertainties in the new CMIP5 climate model projections *Nat. Clim. Change* **3** 369–73
- [14] Stive M J F, Aarninkhof S G J, Hamm L, Hanson H, Larson M, Wijnberg K M, Nicholls R J and Capobianco M

- 2002 Variability of shore and shoreline evolution *Coast. Eng.* **47** 211–35
- [15] Huppert K L, Perron J T and Ashton A D 2020 The influence of wave power on bedrock sea-cliff erosion in the Hawaiian Islands *Geology* **48** 499–503
- [16] Hurst M D, Rood D H, Ellis M A, Anderson R S and Dornbusch U 2016 Recent acceleration in coastal cliff retreat rates on the south coast of Great Britain *Proc. Natl Acad. Sci.* **113** 13336–41
- [17] Storlazzi C D et al 2018 Most atolls will be uninhabitable by the mid-21st century because of sea-level rise exacerbating wave-driven flooding *Sci. Adv.* **4** 4
- [18] Earlie C S, Young A P, Masselink G and Russell P E 2015 Coastal cliff ground motions and response to extreme storm waves *Geophys. Res. Lett.* **42** 847–54
- [19] Taherkhani M, Vitousek S, Barnard P L, Frazer N, Anderson T R and Fletcher C H 2020 Sea-level rise exponentially increases coastal flood frequency *Sci. Rep.* **10** 6466
- [20] Vitousek S, Barnard P L, Fletcher C H, Frazer N, Erikson L and Storlazzi C D 2017 Doubling of coastal flooding frequency within decades due to sea-level rise *Sci. Rep.* **7** 1399
- [21] Klein Tank A M G et al 2009 Climate Data and Monitoring WCDMP-No. 72 WMO/TD- No. 1500 Guidelines on analysis of extremes in a changing climate in support of informed decisions for adaptation (World Meteorological Organization (WMO))
- [22] Feron S et al 2019 Observations and projections of heat waves in South America *Sci. Rep.* **9** 8173
- [23] Hartmann D L et al 2013 Observations: atmosphere and surface *Climate Change 2013: The Physical Science Basis. Contribution of Working Group I to the Fifth Assessment Report of the Intergovernmental Panel on Climate Change* ed T F Stocker, D Qin, G-K Plattner, M Tignor, S K Allen, J Boschung, A Nauels, Y Xia, V Bex and P M Midgley (Cambridge: Cambridge University Press)
- [24] Morim J et al 2020 A global ensemble of ocean wave climate projections from CMIP5-driven models *Sci. Data* **7** 105
- [25] Morim J et al 2019 Robustness and uncertainties in global multivariate wind-wave climate projections *Nat. Clim. Change* **9** 711–8
- [26] Hersbach H et al 2020 The ERA5 global reanalysis *Q. J. R. Meteorol. Soc.* **146** 1999–2049
- [27] Taylor K E 2001 Summarizing multiple aspects of model performance in a single diagram *J. Geophys. Res. Atmos.* **106** 7183–92
- [28] Randall D A et al 2007 Climate models and their evaluation *Climate Change 2007: The Physical Science Basis. Contribution of Working Group I to the Fourth Assessment Report of the Intergovernmental Panel on Climate Change* ed S Solomon, D Qin, M Manning, Z Chen, M Marquis, K B Averyt, M Tignor and H L Miller (Cambridge: Cambridge University Press)
- [29] Flato G J et al 2013 Evaluation of climate models *Climate Change 2013: The Physical Science Basis. Contribution of Working Group I to the Fifth Assessment Report of the Intergovernmental Panel on Climate Change* ed T F Stocker, D Qin, G-K Plattner, M Tignor, S K Allen, J Boschung, A Nauels, Y Xia, V Bex and P M Midgley (Cambridge: Cambridge University Press)
- [30] Bidlot J, Lemos G and Semedo S 2019 ERA5 reanalysis & ERA5 based ocean wave hindcast *2nd Int. Workshop on Waves, Storm Surges, and Coastal Hazards*
- [31] Hemer M A, Katzfey J and Trenham C E 2013 Global dynamical projections of surface ocean wave climate for a future high greenhouse gas emission scenario *Ocean Model.* **70** 221–45
- [32] Bricheno L M and Wolf J 2018 Future wave conditions of Europe, in response to high-end climate change scenarios *J. Geophys. Res. Oceans* **123** 8762–91
- [33] Perez J, Menendez M and Losada I J 2017 GOW2: a global wave hindcast for coastal applications *Coast. Eng.* **124** 1–11
- [34] Shimura T, Mori N and Hemer M A 2016 Variability and future decreases in winter wave heights in the Western North Pacific *Geophys. Res. Lett.* **43** 2716–22
- [35] Morim J, Hemer M, Andutta F, Shimura T and Cartwright N 2020 Skill and uncertainty in surface wind fields from general circulation models: intercomparison of bias between AGCM, AOGCM and ESM global simulations *Int J. Climatol.* **40** 2659–73
- [36] Tebaldi C, Arblaster J M and Knutti R 2011 Mapping model agreement on future climate projections *Geophys. Res. Lett.* **38** L23701
- [37] Fogt R L and Marshall G J 2020 The southern annular mode: variability, trends, and climate impacts across the Southern Hemisphere *WIREs Clim. Change* **11** e652
- [38] Marshall G J 2003 Trends in the Southern annular mode from observations and reanalyses *J. Clim.* **16** 4134–43
- [39] Sillmann J, Kharin V V, Zhang X, Zwiers F W and Bronaugh D 2013 Climate extremes indices in the CMIP5 multimodel ensemble: part 1. model evaluation in the present climate *J. Geophys. Res. Atmos.* **118** 1716–33
- [40] Karnauskas K B, Lundquist J K and Zhang L 2018 Southward shift of the global wind energy resource under high carbon dioxide emissions *Nat. Geosci.* **11** 38–43
- [41] Kar-Man Chang E 2018 CMIP5 projected change in northern hemisphere winter cyclones with associated extreme winds *J. Clim.* **31** 6527–42
- [42] Chang E K M 2017 Projected significant increase in the number of extreme extratropical cyclones in the Southern Hemisphere *J. Clim.* **30** 4915–35
- [43] Chang E K M, Guo Y and Xia X 2012 CMIP5 multimodel ensemble projection of storm track change under global warming *J. Geophys. Res.* **117** D23118
- [44] Marshall A, Hemer M A, Hendon H H and McInnes K L 2018 Southern annular mode impacts on global ocean surface waves *Ocean Model.* **129** 58–74
- [45] Hemer M, Fan Y, Mori N, Semedo A and Wang X L 2013 Projected changes in wave climate from a multi-model ensemble *Nat. Clim. Change* **3** 471–6
- [46] Swart N C, Fyfe J C, Gillett N and Marshall G J 2015 Comparing trends in the Southern annular mode and surface westerly jet *J. Clim.* **28** 8840–59
- [47] Zheng F, Li J, Clark R T and Nnamchi H C 2013 Simulation and projection of the Southern Hemisphere annular mode in CMIP5 models *J. Clim.* **26** 9860–79
- [48] Gillett N P and Fyfe J C 2013 Annular mode changes in the CMIP5 simulations *Geophys. Res. Lett.* **40** 1189–93
- [49] Almar R, Kestenare E, Reyns J, Jouanno J, Anthony E J, Laibi R, Hemer M, Du Penhoat Y and Ranasinghe R 2015 Response of the bight of benin (Gulf of Guinea, West Africa) coastline to anthropogenic and natural forcing, Part1: wave climate variability and impacts on the longshore sediment transport *Cont. Shelf Res.* **110** 48–59
- [50] Silva R et al 2014 Present and future challenges of coastal erosion in Latin America *J. Coast. Res.* **71** 1–16
- [51] Albert S, Leon J X, Grinham A R, Church J A, Gibbs B R and Woodroffe C D 2016 Interactions between sea-level rise and wave exposure on reef island dynamics in the Solomon Islands *Environ. Res. Lett.* **11** 054011
- [52] Harley M D, Turner I L, Kinsela M A, Middleton J H, Mumford P J, Splinter K D, Phillips M S, Simmons J A, Hanslow D J and Short A D 2017 Extreme coastal erosion enhanced by anomalous extratropical storm wave direction *Sci. Rep.* **7** 6033
- [53] Timmermans B, Stone D, Wehner M and Krishnan H 2017 Impact of tropical cyclones on modeled extreme wind-wave climate *Geophys. Res. Lett.* **44** 1393–401
- [54] Cooper J A G et al 2020 Sandy beaches can survive sea-level rise *Nat. Clim. Change* **10** 993–95